Solid Freeform Fabrication 2023: Proceedings of the 34th Annual International Solid Freeform Fabrication Symposium – An Additive Manufacturing Conference
Reviewed Paper

INVESTIGATION OF MULTI-MATERIAL LIQUID METAL JETTING WITH COPPER MATERIALS

M. Ploetz*, F. Heckmeier, B. Kirchebner, W. Volk and P. Lechner

Technical University of Munich, Germany, TUM School of Engineering and Design, Department of Mechanical Engineering, Chair of Metal Forming and Casting

*Corresponding author: maximilian.ploetz@tum.de

Abstract

Technical parts are typically subject to various requirements that may conflict with each other. Multi-material parts can be a way to overcome such conflicting goals. Liquid Metal Jetting (LMJ) can be a promising additive manufacturing process for the production of multi-material copper parts with high geometric complexity. Since LMJ builds up a part droplet by droplet, there are no mixed powders after printing. In addition, LMJ offers the possibility of changing materials from droplet to droplet. In previous studies, we have shown that it is possible to produce copper alloy parts using LMJ. In this work, we produced multi-material copper specimens at different process parameters to investigate the manufacturing of multi-material copper parts. The investigations show that the quality of the compound and the microstructure depend significantly on the thermal process parameters used.

Keywords: Material Jetting, Liquid Metal Jetting, Copper Alloys, Multi-Material Parts

Introduction

Materials often differ considerably in their properties, e.g., in terms of mechanical strength, density, corrosion behavior, or thermal and electrical conductivity. As a result, there is often a conflict of interest when selecting a material for a part. Combining different materials with different properties in a multi-material part can be a possibility to solve such conflicts of interest. Conventional manufacturing processes often require several steps to produce such multi-material parts [1] and are limited in design freedom. Additive manufacturing (AM) processes offer the potential to produce highly complex parts with locally adapted properties without the disadvantages of conventional processes [2]. The material can be adjusted by the local adaptation of properties such as mechanical strength, biocompatibility, or part color [3]. In recent years, many studies have investigated the production of multi-material parts using various AM processes. One AM process for producing multi-material parts is material jetting (MJT). In MJT, droplets of the build material are created using a print head and deposited on a build platform [4]. On the build platform, the droplets solidify, e.g., by cooling or by exposure to light. A part can be built up layer by layer by joining the droplets. Since it is possible to use several print heads, which can be filled with different build materials, MJT offers considerable potential for producing multi-material parts [5]. Multi-material MJT is already used to produce polymer parts [4]. By processing a soft and hard polymer, Tee et al. produced a part with improved mechanical properties using MJT [6]. Another application of multi-material MJT is shown by Inoue et al., who produced a multi-colored bone model [7]. By alternating the build material's colors, a bone model could be created that can be used as an anatomy illustration model. Previous studies on producing parts from one or more

materials using MJT have been limited primarily to non-metallic materials. In recent years, the production of metallic parts using MJT has also become the focus of research and industry. In MJT with metallic materials, so-called Liquid Metal Jetting (LMJ), the build material is melted in a print head and ejected droplet by droplet through a nozzle. A wire can be used as raw material. The ejected droplets are deposited on a build platform, where they solidify. Depending on the metallic material used, significantly higher processing temperatures are needed in the LMJ process compared to MJT with polymers.

Different metallic materials can be processed via LMJ. A detailed overview of the materials investigated to date was provided by Ansell [8]. Initial investigations were carried out with low-melting materials based on tin and aluminum. Orme and Smith produced and characterized the first aluminum parts via LMJ [9]. The heat transfer during the printing of vertical columns of aluminum was investigated by Fang et al., both analytically and based on practical tests. Column-shaped aluminum test specimens were produced at different process temperatures. It was found that the temperature of the uppermost droplet of the column must be slightly below the melting point of the build material to obtain good bonding of the newly impinging droplet. Exceeding the melting temperature in the contact area led to the destruction of the already-printed column [10]. Chao et al. produced four rectangular aluminum test specimens at different thermal process parameters. Here, too-high temperatures in the contact area of the newly impinging droplets also led to the loss of the already printed geometry. On the other hand, low temperatures increased pores in the part [11]. Further investigations on the influence of thermal process parameters on the printing result during the processing of aluminum materials were carried out by Zuo et al. [12] and Himmel et al. [13]. In particular, the parameters' influence on the mechanical properties were investigated.

In addition to aluminum as a build material, the processing of copper and copper alloys using LMJ has also been investigated. Zhong et al. studied the process of generating copper droplets with a pneumatically actuated generator. After identifying suitable parameters for stable droplet generation, several copper droplets could be deposited on each other, and a columnar part could be produced [14]. In further work by Zhong et al., the pneumatic pressure signal arriving in the crucible was measured and subsequently used as an input variable for simulating the droplet generation [15]. Ploetz et al. produced test specimens from a copper-tin bronze using LMJ at different droplet and build platform temperatures and carried out a mechanical characterization of the parts. Specimens printed at a build platform temperature close to the solidus temperature of the material showed the highest values for tensile strength and uniform elongation within the scope of the investigations [16].

To the authors' knowledge, processing more than one material in the LMJ process to produce multi-material parts has not yet been investigated. This paper will examine the production of multi-material parts using two copper materials. Pure copper has high thermal and electrical conductivity and is often used for electrical components or cooling devices [17]. Adding tin reduces thermal and electrical conductivity but improves the material's hardness, mechanical strength, and corrosion resistance. By combining the two materials in one part, both advantages of the materials can be used specifically at the location of the required load.

It is known from numerous preliminary studies that the quality of the droplet bonding and, thus, the quality of the parts is significantly influenced by the thermal conditions during the droplet deposition. Consequently, the thermal process variables, essentially the build platform temperature,

must be adapted to the material to be processed. These are often slightly below the solidus temperatures of the materials. However, when processing more than one material within one printing process, there are limitations in adjusting the build platform temperature. The lower melting material limits the maximum build platform temperature, as excessively high substrate temperatures can lead to renewed melting of the already deposited material and, thus, to the destruction of the structure of the parts. Especially with material combinations where the individual materials have very different solidus temperatures, possible problems may be expected. In the context of this work, this problem is to be investigated based on multi-material parts consisting of two copper-tin bronzes with different tin contents and, thus, different solidus temperatures. The investigation is carried out using rectangular test specimens. The copper-tin bronzes CuSn1 and CuSn8 are used as build materials.

At the beginning of the paper, the LMJ test stand used for the fabrication of the test specimens and the build materials used are presented. This is followed by the presentation of the specimen geometry and the description of the experimental procedure. Finally, the results are shown using micrographs of the produced multi-material parts.

Material and Methods

Test stand for LMJ

The samples for this work are fabricated on a LMJ test stand with a high-temperature print head and a heated build platform. Figure 1 shows the LMJ test stand used.

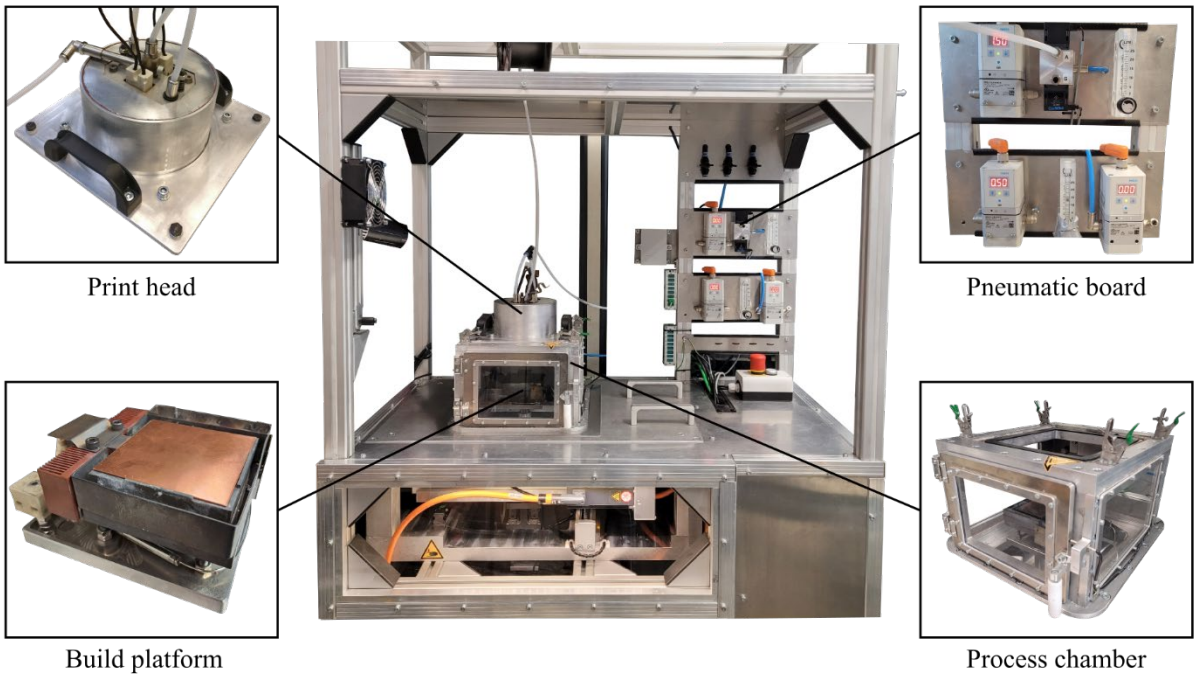

Figure 1: MJT test stand for processing aluminum, copper, and salt as support structures.

In the center of the test stand is the process chamber in which the part is built. Various high-temperature print heads can be mounted on the process chamber to generate droplets. The system can process aluminum materials, salts as a support structure, and copper materials. All print heads

generate the droplets using a pneumatic pressure surge. During the printing process and the cooling phase of the printed part, the process chamber can be purged with nitrogen. The flooding of the process chamber reduces the oxidation of processed material.

Below the static print head is the heated build platform. This platform can be moved within the process chamber. The droplets produced by the print head are deposited on a substrate plate attached to the top of the build platform. The substrate plate, including the manufactured part, can be detached from the build platform after printing. Substrate plates made of different materials can be used. The substrate plate can be heated to a temperature of 1020 °C via a heating element installed in the build platform. The build platform can be moved in the x-y direction during printing to produce a layer of the part. After creating a layer, the build platform can be lowered in the z-direction.

A single print head is used to produce test specimens, where a material change only occurs from one layer to the next. This single print head has only one crucible and nozzle for generating droplets. Figure 2 shows schematically the components of the high-temperature print head.

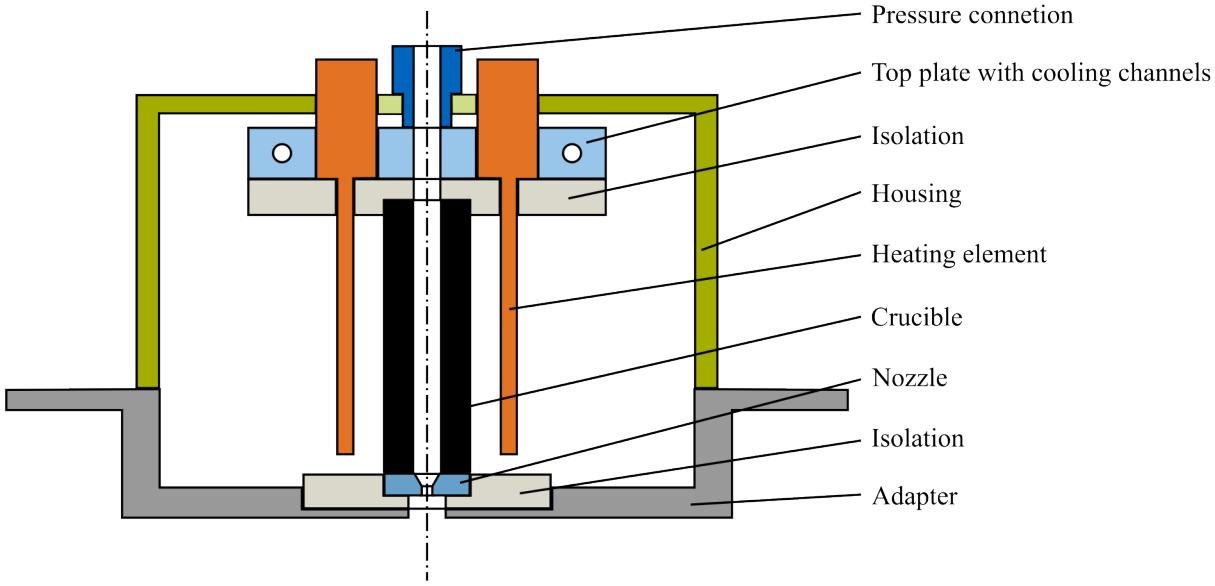

Figure 2: Schematic illustration of the components of the high-temperature print head.

In the center of the print head is a graphite crucible used to melt and store the build material. Two side-mounted heating elements heat the crucible via radiation. This allows the crucible to be heated in a controlled manner up to a maximum temperature of 1200 °C. The area around the graphite crucible is flooded with nitrogen to prevent the crucible from burning off. A nozzle made of graphite is attached to the underside of the tubular crucible. In the center of the nozzle is a 500 µm diameter orifice. At the top of the crucible, the wire-shaped build material can be fed into the crucible. The wire is melted in the crucible, and a defined amount of melt is stored. Adding wire during the printing process keeps the height of the melt level constant. In the initial state, no melt flows out of the nozzle orifice due to the surface tension. A pneumatic pressure surge is applied to the melt from above to create droplets. As with the flooding of the process chamber and the print head in the crucible area, nitrogen is used as the process gas for droplet generation. The

level of the applied pressure pulse and the time for which the pressure pulse acts on the melt are controlled by a programmable logic controller (PLC). The PLC also controls the temperatures of the build platform and the crucible, the process chamber's flooding, and the build platform movement. The temperature of the crucible is recorded via thermocouples. An oxygen sensor is installed in the process chamber to detect the oxygen content.

Build material

In this work, multi-material parts consisting of CuSn1 and CuSn8 are investigated. The raw materials for producing the multi-material parts are copper-tin bronze CuSn8 and copper Cu-ETP (Wieland-Werke AG, Ulm, Germany). The copper-tin bronze CuSn8 is in the form of a wire with a diameter of 2 mm. This copper-tin-bronze has a liquidus temperature of 1040 °C and a solidus temperature of 860 °C. The diameter of the Cu-ETP wire is 1.2 mm. The material has a melting point of 1083 °C. To prepare the material CuSn1, the wires of CuSn8 and Cu-ETP are proportionally melted and mixed in the crucible of the print head. The chemical composition of the used build materials CuSn8 and CuSn1 are listed in Table 1 and Table 2. The three elements with the highest concentration determined are listed in each case. Using a printed test specimen, the material composition is determined by spark spectrometry (FOUNDRY-MASTER, Worldwide Analytical Systems GmbH, Kleve, Germany).

Table 1: Composition of a CuSn8 sample produced via LMJ, determined by optical emission spectroscopy. All values in %.

Element	Concentration in measurement 1	Concentration in measurement 2
Cu	92.6	92.9
Sn	6.83	6.97
P	0.112	0.039

Table 2: Composition of a CuSn1 sample produced via LMJ, determined by optical emission spectroscopy. All values in %.

Element	Concentration in measurement 1	Concentration in measurement 2
Cu	99.2	99.2
Sn	0.74	0.71
P	0.0015	< 0.0010

Geometry and printing strategy

Rectangular test specimens were produced to investigate the LMJ of multi-material copper parts. These consist of eight layers on top of each other, whereby a material change only takes place in the z-direction. First, four layers of material 1 are produced. Then, four more layers of material 2 are printed. One layer consists of four parallel lines. Each line consists of 15 droplets. The distance between the droplets of a line is 0.8 mm. The distance between the individual lines is 0.75 mm. Figure 3 shows the test geometry schematically.

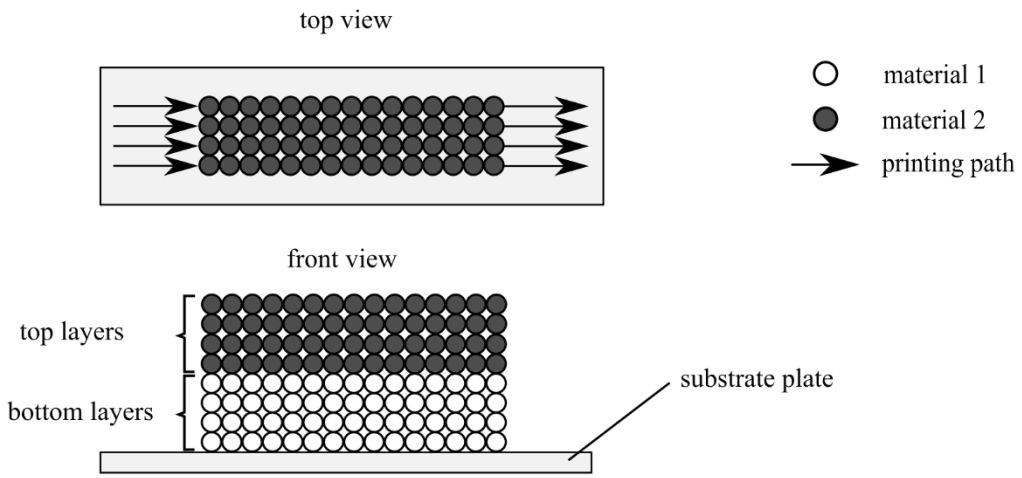

Figure 3: Schematic illustration of the printing strategy.

Experimental procedure

Figure 4 shows the procedure for manufacturing and evaluating the test specimens.

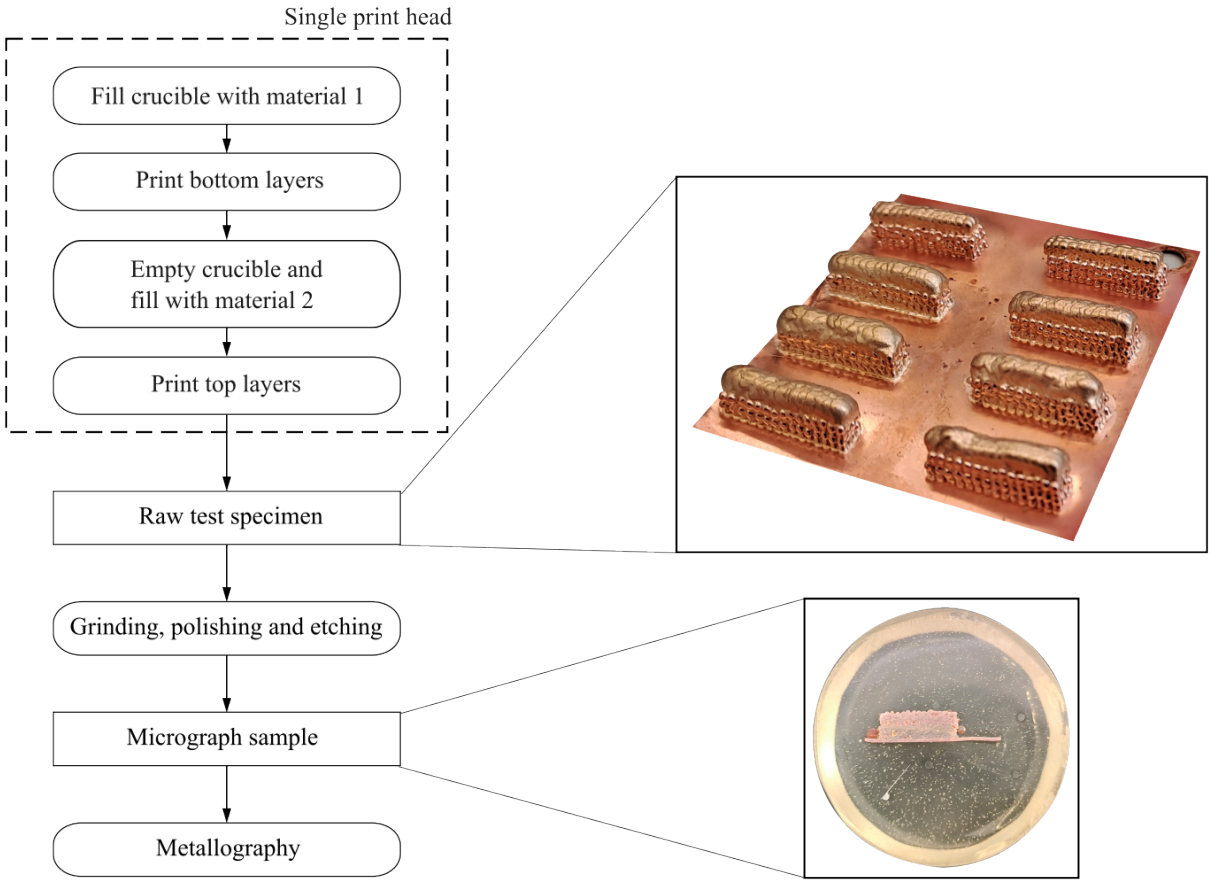

Figure 4: Experimental procedure.

The flow diagram shows the manufacturing and evaluation process of the rectangular test specimens with one-dimensional material change in the z-direction. These test specimens are produced with a single print head. Since this print head contains only one crucible in which the raw material is melted and stored, the rectangular test specimens are produced in two steps. In the first step, the crucible is filled with material 1, and the bottom layers of the test specimen are printed. The temperature of the build platform is adapted to the material to be processed to create these layers. For the manufacturing of CuSn8, the build platform temperature is $T_{platform}$ = 850 ° for CuS1 $T_{platform}$ = 980 °C. Afterward, material 1, still in the crucible, is ejected outside the specimen to be printed, and the crucible is emptied. The empty crucible is then filled with material 2, and the remaining layers of the test specimen are produced with material 2. The top layers are printed once at a build platform temperature of $T_{platform}$ = 850 °C and once at a build platform temperature of $T_{platform}$ = 980 °C. By combining two different material combinations for CuSn1 or CuSn8 as top layers and the two build platform temperatures investigated, four configurations will be investigated. Three specimens are printed for each configuration. For each configuration, one characteristic specimen is selected to be represented in this paper.

After the printing process, the rectangular specimen is prepared for metallography. The specimens are first embedded in epoxy resin (Kulzer GmbH, Hanau, Germany). Then, the specimens are ground and polished. The polished surface is etched and then examined using reflected light microscopy. An AxioCam MRc5 camera system, which is part of the reflected-light microscope (Axioplan 2, Carl Zeiss MicroImaging GmbH, Goettingen, Germany), is used to analyze the material microstructure based on micrographs.

Table 3 shows the process parameters used to produce the test specimens. The droplet temperature for both materials is chosen to be $T_{droplet,\ CuSn1}$ = $T_{droplet,\ Cusn8}$ = 1130 °C to avoid any influence of the droplet temperatures on the print result. The print head has a nozzle with an orifice of 500 µm. This setup produces droplets of CuSn1 and CuSn8 with an average diameter of 0.9 mm. Individual droplets can have a deviation of up to 10% from the average droplet diameter. The frequency to eject droplets is 50 Hz. The residual oxygen content is measured with an oxygen sensor installed in the process chamber. The content is < 50 ppm during part manufacturing and the cooling process. The temperature of the build platform is examined at two levels. A temperature of $T_{platform}$ = 850 °C is used as the suitable temperature for processing CuSn8. The temperature assumed to be suitable for processing CuSn1 is chosen to be $T_{platform}$ = 980 °C.

Table 3: Process Parameters used.

Parameter	**Symbol**	**Values**
Temperature droplet CuSn1	$T_{droplet,\ CuSn1}$	1130 °C
Temperature droplet CuSn8	$T_{droplet,\ CuSn8}$	1130 °C
Temperature platform	$T_{platform}$	850 °C / 980 °C
Droplet diameter CuSn1	$d_{droplet,\ CuSn1}$	0.9 mm
Droplet diameter CuSn8	$d_{droplet,\ CuSn8}$	0.9 mm
Deposition rate	$f_{deposition}$	50 Hz
Oxygen in process chamber	c_{oxygen}	< 50 ppm
Speed of the build platform during droplet deposition	$v_{platform}$	$40\,\frac{\mathrm{mm}}{\mathrm{s}}$

Results and Discussion

Figure 5 shows the etched micrographs of the four produced test specimens. In the top row, figures 5(a) and 5(b) show the micrographs of the test specimens for which four layers of CuSn8 were produced first and then four layers of CuSn1. The bottom row shows in figures 5(c) and 5(d) the micrographs of the parts where CuSn8 was printed on CuSn1. Below each micrograph, the respective temperatures of the build platform during the production of the bottom and top layers are shown. The top layers in figure 5(a) and 5(c) were produced at a build platform temperature of $T_{platform}$ = 850 °C. In figure 5(b) and 5(d), the build platform temperature for the production of the top layers is $T_{platform}$ = 980 °C. The bottom layers were each produced at suitable temperatures. For CuSn8, the suitable temperature was set at $T_{platform}$ = 850 °C and for CuSn1, at $T_{platform}$ = 980 °C.

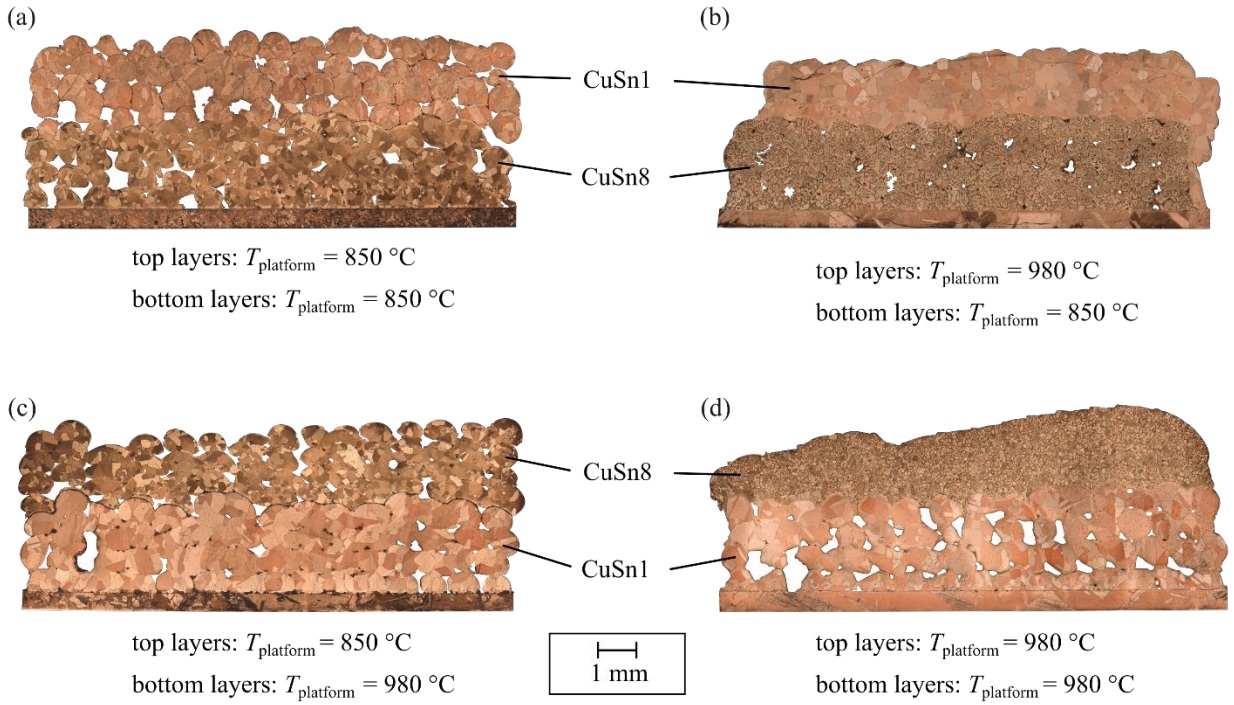

Figure 5: Micrographs of the multi-material parts of CuSn1 and CuSn8 produced at different platform temperatures.

The micrographs in Figures 5(a) and 5(b), where CuSn1 was printed on CuSn8, show different microstructure and pore amounts for the different temperatures used to print the top layers. In Figure 5(b), the CuSn1 layers have fewer pores than the CuSn1 layers of the part in Figure 5(a). The reason for this is the better droplet bonding due to the higher temperatures of the build platform during droplet deposition. In addition, larger grains tend to be observed in the microstructure of the CuSn1 material of the part in Figure 5(b).

A difference in the microstructure of the bottom layers of CuSn8 can also be seen when comparing the micrographs shown in Figure 5(a) and 5(b). The bottom layers in Figure 5(b) show the segregation of the CuSn8 material. No segregation can be detected in the bottom layers of the part produced at a platform temperature of $T_{platform}$ = 850 °C shown in Figure 5(a).

The micrographs in figures 5(c) and 5(d), where CuSn8 was printed on CuSn1, also differ significantly depending on the temperatures used to produce the top layers. The top layers out of CuSn8 again show segregation of the material in the part shown in Figure 5(d), which has a platform temperature of $T_{platform}$ = 980 °C during the production of the top layers. In addition, the shape of the individual droplets is no longer recognizable. The part geometry shows a deviation from the intended rectangular shape. The rectangular shape is still preserved in the part shown in Figure 5(c), where the top layers were produced at a temperature of $T_{platform}$ = 850 °C. However, this part has more pores in the top layers. The bottom layers of CuSn1 have a similar microstructure for both temperatures used to produce the top layers. The part shown in Figure 5(d) produced at the higher temperature of $T_{platform}$ = 980 °C shows a slight enlargement of the grains due to the higher platform temperature during the printing of the top layers.

The micrographs show that the droplets of the top layers fuse better together at the higher platform temperature $T_{platform}$ = 980 °C examined. If CuSn1 is printed on CuSn8, this causes a reduction in the porosity present in the part and thus tends to improve the part quality compared to the build platform temperature of $T_{platform}$ = 850 °C. If the top layers are made of CuSn8 and a build platform temperature of $T_{platform}$ = 980 °C is used to produce the top layers, this leads to an unwanted partial loss of the part geometry. The reason for this is the re-melting of the already deposited CuSn8 drops. In addition, a segregation of the CuSn8 material can be observed at the higher build platform temperature used to produce the top layers.

Conclusion

In this paper, we demonstrated the manufacturability of multi-material parts made of copper alloys via LMJ. Using rectangular test specimens with a material change in the z-direction, the influence of the selected build platform temperature on the properties of the material structure, the porosity, and the part geometry was investigated. At the high temperature investigated during the production of the top layers, the droplets fuse better. If CuSn1 is used as the material for the top layers, the part quality improves. With CuSn8 as the material for the top layers, the part geometry is partially lost. These observations show the challenges in the production of metallic multi-material parts. Different substrate temperatures are required to produce a high-quality part depending on the build material. However, the material with the lower solidus temperature limits the temperature of the build platform. When processing the material with a higher solidus temperature, porosity can occur due to the low substrate temperature.

To solve this problem, future work will investigate ways to locally increase the substrate temperature to realize good droplet bonding even at low build platform temperatures. Possible approaches could be to adjust the droplet size, the printing frequency, and the printing pattern. In addition, a characterization of the interface between the two materials will be performed.

Acknowledgments

This research was supported by the Arbeitsgemeinschaft industrieller Forschungsvereinigungen (AiF, Entrepreneurial innovation) -IGF project-ID 21553 N. We want to thank Wieland-Werke AG, for providing the semi-finished product needed to conduct this research. Furthermore, we would like to thank Corinna Sutter for her experimental support.

References

1. Bandyopadhyay A, Heer B (2018) Additive manufacturing of multi-material structures. Materials Science and Engineering: R: Reports 129:1–16. https://doi.org/10.1016/j.mser.2018.04.001
2. Hasanov S, Alkunte S, Rajeshirke M et al. (2022) Review on Additive Manufacturing of Multi-Material Parts: Progress and Challenges. JMMP 6:4. https://doi.org/10.3390/jmmp6010004
3. Gülcan O, Günaydın K, Tamer A (2021) The State of the Art of Material Jetting—A Critical Review. Polymers 13:2829. https://doi.org/10.3390/polym13162829
4. Wohlers T, Campbell RI, Diegel O et al. (2019) Wohlers report 2019: 3D printing and additive manufacturing state of the industry. Wohlers Associates, Fort Collins, Colo.
5. Nazir A, Gokcekaya O, Md Masum Billah K et al. (2023) Multi-material additive manufacturing: A systematic review of design, properties, applications, challenges, and 3D printing of materials and cellular metamaterials. Materials & Design 226:111661. https://doi.org/10.1016/j.matdes.2023.111661
6. Tee YL, Tran P, Leary M et al. (2020) 3D Printing of polymer composites with material jetting: Mechanical and fractographic analysis. Additive Manufacturing 36:101558. https://doi.org/10.1016/j.addma.2020.101558
7. Inoue M, Freel T, van Avermaete A et al. (2020) Color Enhancement Strategies for 3D Printing of X-ray Computed Tomography Bone Data for Advanced Anatomy Teaching Models. Applied Sciences 10:1571. https://doi.org/10.3390/app10051571
8. Ansell TY (2021) Current Status of Liquid Metal Printing. JMMP 5:31. https://doi.org/10.3390/jmmp5020031
9. Orme M, Smith RF (2000) Enhanced Aluminum Properties by Means of Precise Droplet Deposition. Journal of Manufacturing Science and Engineering 122:484–493. https://doi.org/10.1115/1.1285914
10. Fang M, Chandra S, Park CB (2009) Heat Transfer During Deposition of Molten Aluminum Alloy Droplets to Build Vertical Columns. Journal of Materials Processing Technology 131:62. https://doi.org/10.1115/1.3156782
11. Chao Y-p, Qi L-h, Zuo H-s et al. (2013) Remelting and bonding of deposited aluminum alloy droplets under different droplet and substrate temperatures in metal droplet deposition manufacture. International Journal of Machine Tools and Manufacture 69:38–47. https://doi.org/10.1016/J.IJMACHTOOLS.2013.03.004
12. Zuo H, Li H, Qi L et al. (2016) Influence of Interfacial Bonding between Metal Droplets on Tensile Properties of 7075 Aluminum Billets by Additive Manufacturing Technique. Journal of Materials Science & Technology 32:485–488. https://doi.org/10.1016/j.jmst.2016.03.004
13. Himmel B, Rumschoettel D, Volk W (2019) Tensile properties of aluminium 4047A built in droplet-based metal printing. RPJ 25:427–432. https://doi.org/10.1108/RPJ-02-2018-0039
14. Zhong SY, Le Qi H, Luo J et al. (2012) Parameters Study on Generation of Uniform Copper Droplet by Pneumatic Drop-on-Demand Technology. AMR 430-432:781–784. https://doi.org/10.4028/www.scientific.net/AMR.430-432.781
15. Zhong S-y, Qi L-h, Luo J et al. (2014) Effect of process parameters on copper droplet ejecting by pneumatic drop-on-demand technology. Journal of Materials Processing Technology 214:3089–3097. https://doi.org/10.1016/j.jmatprotec.2014.07.012

16. Ploetz M, Kirchebner B, Volk W et al. (2023) Influence of thermal process parameters on the properties of material jetted CuSn8 components. Materials Science and Engineering: A 871:144869. https://doi.org/10.1016/j.msea.2023.144869
17. Davis JR (ed) (2001) Copper and copper alloys. ASM specialty handbook. ASM International, Materials Park, Ohio